Cell Reports
Report

Aβ Secretion and Plaque Formation Depend on Autophagy

Per Nilsson,[1,*] Krishnapriya Loganathan,[1] Misaki Sekiguchi,[1] Yukio Matsuba,[1] Kelvin Hui,[2] Satoshi Tsubuki,[1] Motomasa Tanaka,[2] Nobuhisa Iwata,[3] Takashi Saito,[1] and Takaomi C. Saido[1,*]
[1]Laboratory for Proteolytic Neuroscience, RIKEN Brain Science Institute, 2-1 Hirosawa, Wako, Saitama 351-0198, Japan
[2]Laboratory for Protein Conformation Diseases, RIKEN Brain Science Institute, 2-1 Hirosawa, Wako, Saitama 351-0198, Japan
[3]Department of Biotechnology, Graduate School of Biomedical Sciences, Nagasaki University, 1-14 Bunkyo-machi, Nagasaki 852-8521, Japan
*Correspondence: per-nilsson@brain.riken.jp (P.N.), saido@brain.riken.jp (T.C.S.)
http://dx.doi.org/10.1016/j.celrep.2013.08.042

SUMMARY

Alzheimer's disease (AD) is a neurodegenerative disease biochemically characterized by aberrant protein aggregation, including amyloid beta (Aβ) peptide accumulation. Protein aggregates in the cell are cleared by autophagy, a mechanism impaired in AD. To investigate the role of autophagy in Aβ pathology in vivo, we crossed amyloid precursor protein (APP) transgenic mice with mice lacking autophagy in excitatory forebrain neurons obtained by conditional knockout of autophagy-related protein 7. Remarkably, autophagy deficiency drastically reduced extracellular Aβ plaque burden. This reduction of Aβ plaque load was due to inhibition of Aβ secretion, which led to aberrant intraneuronal Aβ accumulation in the perinuclear region. Moreover, autophagy-deficiency-induced neurodegeneration was exacerbated by amyloidosis, which together severely impaired memory. Our results establish a function for autophagy in Aβ metabolism: autophagy influences secretion of Aβ to the extracellular space and thereby directly affects Aβ plaque formation, a pathological hallmark of AD.

INTRODUCTION

Alzheimer's disease (AD) is the major form of dementia in the elderly, characterized by memory loss and cognitive decline. AD brain pathology includes intracellular aggregation of amyloid beta (Aβ) peptide and protein tau and extracellular Aβ plaques (Wirths and Bayer, 2012). Aβ is generated by sequential cleavage of type I transmembrane amyloid precursor protein (APP) by β- and γ-secretases (LaFerla et al., 2007). Mutations in *APP* or the γ-secretase subunits presenilin 1 (*PS1*) and *PS2* cause early-onset familial AD (FAD), thereby tightly linking AD and Aβ. However, FAD cases represent a few percent of all AD cases, and therefore other cellular mechanisms that affect Aβ metabolism likely contribute to the pathology in sporadic AD.

In the AD brain, autophagosomes accumulate in the dystrophic neurites indicating impaired autophagy (Nixon, 2007). Macroautophagy (herein referred to as autophagy; reviewed in Mizushima and Komatsu, 2011 and Harris and Rubinsztein, 2012) controls cellular proteostasis by sequestering and delivering protein aggregates and cellular organelles to lysosomes for degradation. In AD, both the autophagy-inhibitory mammalian target-of-rapamycin (mTOR) signaling and the levels of lysosomal hydrolases are increased (Yang et al., 2011), the latter of which may reflect impaired autophagosomal-lysosomal clearance (Boland et al., 2008). Furthermore, FAD-associated mutations in PS1 disrupt lysosomal proteolysis (Lee et al., 2010a), whereas genetic deletion of the endogenous lysosomal-associated cathepsin inhibitor cystatin B restores lysosomal clearance in autophagy-deficient TgCRND8 mice (Yang et al., 2011). In addition, autophagy sustains axonal homeostasis of neurons (Komatsu et al., 2007) and its absence causes neurodegeneration (Hara et al., 2006; Inoue et al., 2012; Komatsu et al., 2006).

A role for autophagy in Aβ metabolism has been suggested (Boland et al., 2010; Caccamo et al., 2010; Jaeger et al., 2010). For example, autophagosomes generate and contain Aβ (Yu et al., 2005) and oxidative stress-induced autophagy increases Aβ generation (Zheng et al., 2011). Moreover, induction of autophagy by rapamycin in vivo lowers intracellular Aβ levels and improves cognition (Caccamo et al., 2010), and long-term rapamycin treatment reduces plaque load in AD model mice (Majumder et al., 2011). Conversely, heterozygous deletion of autophagy-initiating Beclin1, which is decreased in early AD, increases both intracellular and extracellular Aβ load (Pickford et al., 2008). Endocytosis of exogenous Aβ in turn inhibits autophagy by increasing mTOR signaling (Caccamo et al., 2010).

Although previous studies have linked Aβ metabolism to the degradative function of autophagy, the ultimate effect of genetic deletion of autophagy on Aβ metabolism remained to be elucidated. We therefore generated forebrain excitatory neuron-specific autophagy-deficient APP transgenic mice. This was achieved by conditional knockout of autophagy-related gene 7 (*Atg7*). Unexpectedly, autophagy deficiency drastically reduced

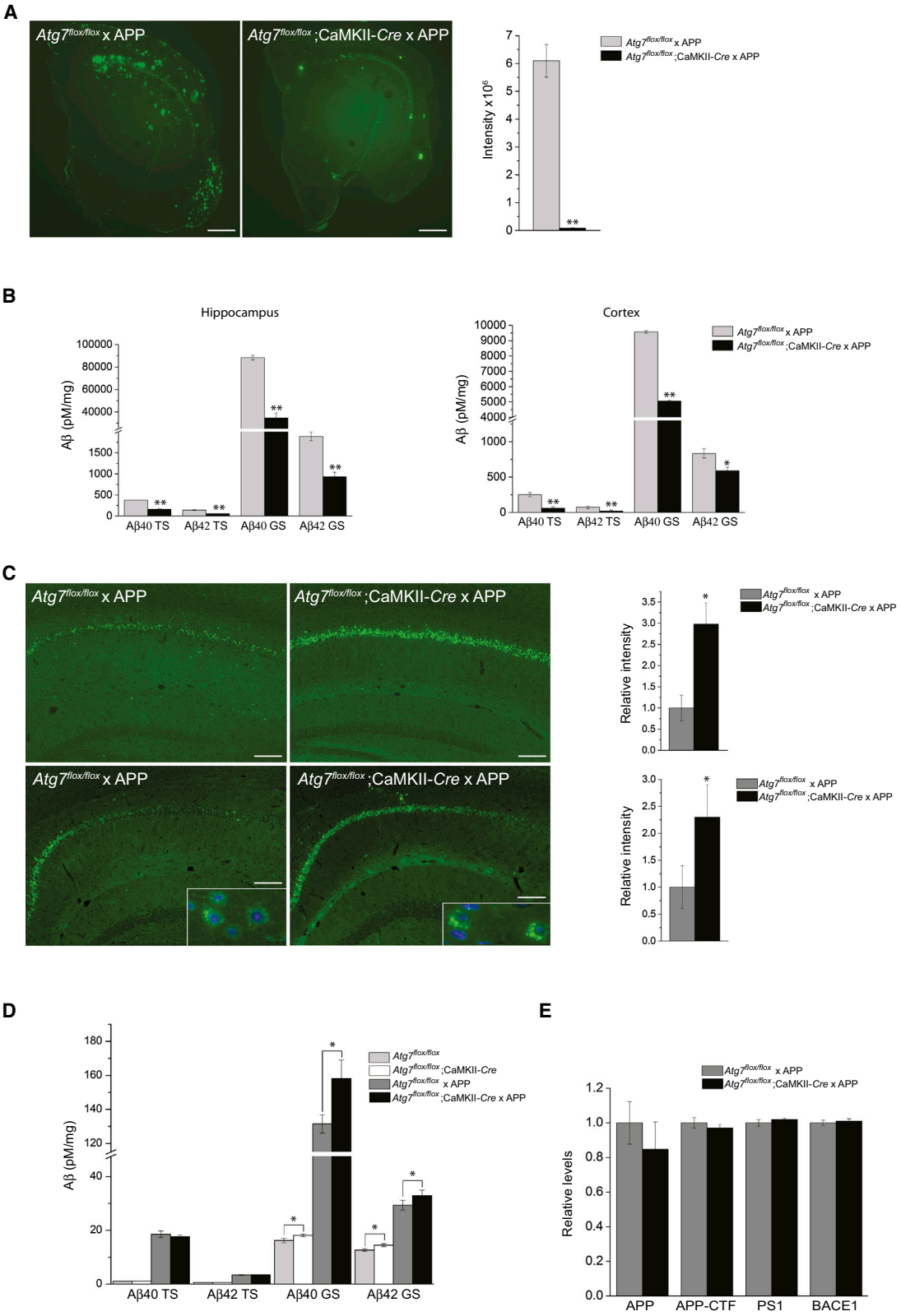

(legend on next page)

the extracellular Aβ plaque load. Through our detailed examination, we have uncovered that the reduced Aβ burden was caused by impaired secretion of Aβ. These data reveal an additional role of autophagy in Aβ metabolism and highlight the importance of autophagy in AD.

RESULTS

Aβ Plaque Formation Is Dependent on Autophagy

To investigate the role of autophagy in Aβ pathology of AD, we generated neuron-specific autophagy-deficient mice by conditionally knocking out the autophagy-essential enzyme Atg7 in excitatory neurons in the mouse forebrain. This was achieved by crossbreeding *Atg7*$^{flox/flox}$ mice (Komatsu et al., 2005) with calcium/calmodulin-dependent protein kinase II (CaMKII)-*Cre* transgenic (Tg) mice. In agreement with previous studies (Komatsu et al., 2006; Inoue et al., 2012) autophagy deficiency led to accumulation of p62/p-S403-p62-positive and polyubiquitinated proteins that formed inclusion bodies in cornu ammonis 1 (CA1), accompanied by accumulation of quality control autophagy-associated histone deacetylase 6 (HDAC6) in CA3 and triggered astrocytosis (Figures S1, S2, and S3).

Next, *Atg7*$^{flox/flox}$; CamKII-*Cre* mice were crossbred with APP23 Tg AD model mouse (herein referred to as APP), and at 20 months of age, Aβ plaque formation was investigated in *Atg7*$^{flox/flox}$ × APP and *Atg7*$^{flox/flox}$; CamKII-*Cre* × APP littermates by Aβ immunostaining. As expected, *Atg7*$^{flox/flox}$ × APP mice exhibited heavy plaque burden at this age. In sharp contrast, Aβ plaque load was drastically reduced upon genetic deletion of *Atg7* (Figure 1A; $p < 0.005$). Consistently, the levels of Tris-soluble (TS) and guanidine-HCl-soluble (GS) Aβ40 and Aβ42 were substantially lowered in *Atg7*$^{flox/flox}$; CamKII-*Cre* × APP mice (Figure 1B; $p < 0.005$). These findings imply that autophagy plays a critical role for Aβ plaque formation.

Autophagy Deficiency Leads to Intracellular Aβ Accumulation

The decreased Aβ plaque load suggested that either Aβ generation is decreased or that Aβ accumulates intracellularly in the autophagy-deficient mice. To elucidate the underlying cause, brain sections of 6-month-old *Atg7*$^{flox/flox}$ × APP and *Atg7*$^{flox/flox}$; CamKII-*Cre* ×APP littermates were immunostained with Aβ specific antibodies, a time point well before Aβ plaque formation starts (Figure S2E; Figure 1C). Interestingly, autophagy deficiency induced intracellular Aβ accumulation in CA1 and cortical pyramidal neurons ($p < 0.05$). Consistently, the levels of both GS-Aβ40 and GS-Aβ42 were slightly but significantly increased in *Atg7*$^{flox/flox}$; CamKII-*Cre* mice compared to *Atg7*$^{flox/flox}$ mice and in *Atg7*$^{flox/flox}$; CamKII-*Cre* × APP mice compared to *Atg7*$^{flox/flox}$ × APP mice (Figure 1D; $p < 0.05$). However, the measured Aβ concentrations were normalized to the wet weight of the brain tissue, and, as described below, autophagy deficiency induces neurodegeneration, which reduces the brain weight by approximately 10% at 6 months of age (data not shown). Therefore, the increased GS-Aβ concentrations most likely reflect both increased intracellular Aβ levels (approximately 10%) as well as reduced brain weight. In addition, the levels of APP, APP C-terminal fragment, PS1, and β-secretase 1 were not altered in autophagy-deficient mice (Figure 1E). In conclusion, autophagy deficiency induces intracellular Aβ accumulation.

Autophagy Influences Secretion of Aβ

The lowered extracellular Aβ plaque burden and the increased intracellular Aβ accumulation indicated that autophagy deficiency impairs secretion of Aβ to extracellular space either through impaired exocytic or excretory mechanisms. Indeed, genetic inhibition of autophagy in cortical/hippocampal primary neurons reduced the extracellular release of endogenous Aβ by 90% (Figure 2A; $p < 0.0001$). Supplementing the autophagy-deficient neurons with Atg7, expressed from a lentivirus to a level similar to that of endogenous Atg7 in autophagy-competent neurons, reactivated autophagy and restored the level of released Aβ to extracellular space to that of autophagy-competent neurons (Figures 2B and 2C; $p < 0.01$). In addition, lenti-Atg7 expression in autophagy-competent neurons increased autophagy and enhanced extracellular Aβ release.

In parallel, wild-type primary neurons were treated with pharmacological activators and inhibitors of autophagy. Low nanomolar concentrations of the mTOR inhibitor rapamycin increased the amount of autophagosomes as measured by LC3 metabolism and p70 phosphorylation and induced Aβ secretion (Figure 2D; $p < 0.01$). In contrast, inhibition of autophagy by spautin-1 significantly reduced extracellular Aβ release ($p < 0.05$), as did inhibition of transport by exposing the neurons to the microtubule destabilizing agent vinblastine ($p < 0.01$). The data obtained by genetically and pharmacologically manipulating autophagy suggest a role for autophagy in intracellular transport and secretion of Aβ. In agreement, Aβ immunostaining of autophagy-deficient neurons revealed substantial accumulation of Aβ in the perinuclear region, whereas significantly less Aβ was transported to the neurites as compared to autophagy-competent neurons (Figure 2E). From these data, we conclude that autophagy influences intracellular transport and secretion of Aβ,

Figure 1. Aβ Plaque Formation Depends on Autophagy

(A) Immunohistological analysis of Aβ plaque (4G8 antibody) in 20-month-old *Atg7*$^{flox/flox}$ × APP and *Atg7*$^{flox/flox}$; CamKII-*Cre* × APP mouse brains. Aβ plaque staining was quantified (n = 4, $^{**}p < 0.005$).

(B) Aβ ELISA measurements of hippocampal and cortical brain homogenates of 20-month-old *Atg7*$^{flox/flox}$ × APP and *Atg7*$^{flox/flox}$; CamKII-*Cre* × APP mice (n = 6, $^{*}p < 0.05$, $^{**}p < 0.005$).

(C) Brain sections of 6-month-old *Atg7*$^{flox/flox}$ × APP and *Atg7*$^{flox/flox}$; CamKI-*Cre* × APP mice were immunostained with N1D-Aβ antibody (upper panels) and Aβ40 antibody (lower panels). Inset shows cortical neurons at 40× magnification. Aβ staining in CA1 was quantified (n = 5, $^{*}p < 0.05$).

(D) Aβ ELISA measurements of hippocampal brain homogenates of 6-month-old mice with genotypes as indicated (n = 6, $^{*}p < 0.05$).

(E) APP, APP-CTF, PS1, and BACE1 levels in hippocampal brain homogenates from 6-month-old mice with genotypes as indicated were determined by quantitative western blot (n = 5, no significant difference).

Scale bars represent 500 μm (A) and 100 μm (C). Data are represented as mean ± SEM. See also Figures S1, S2, and S3.

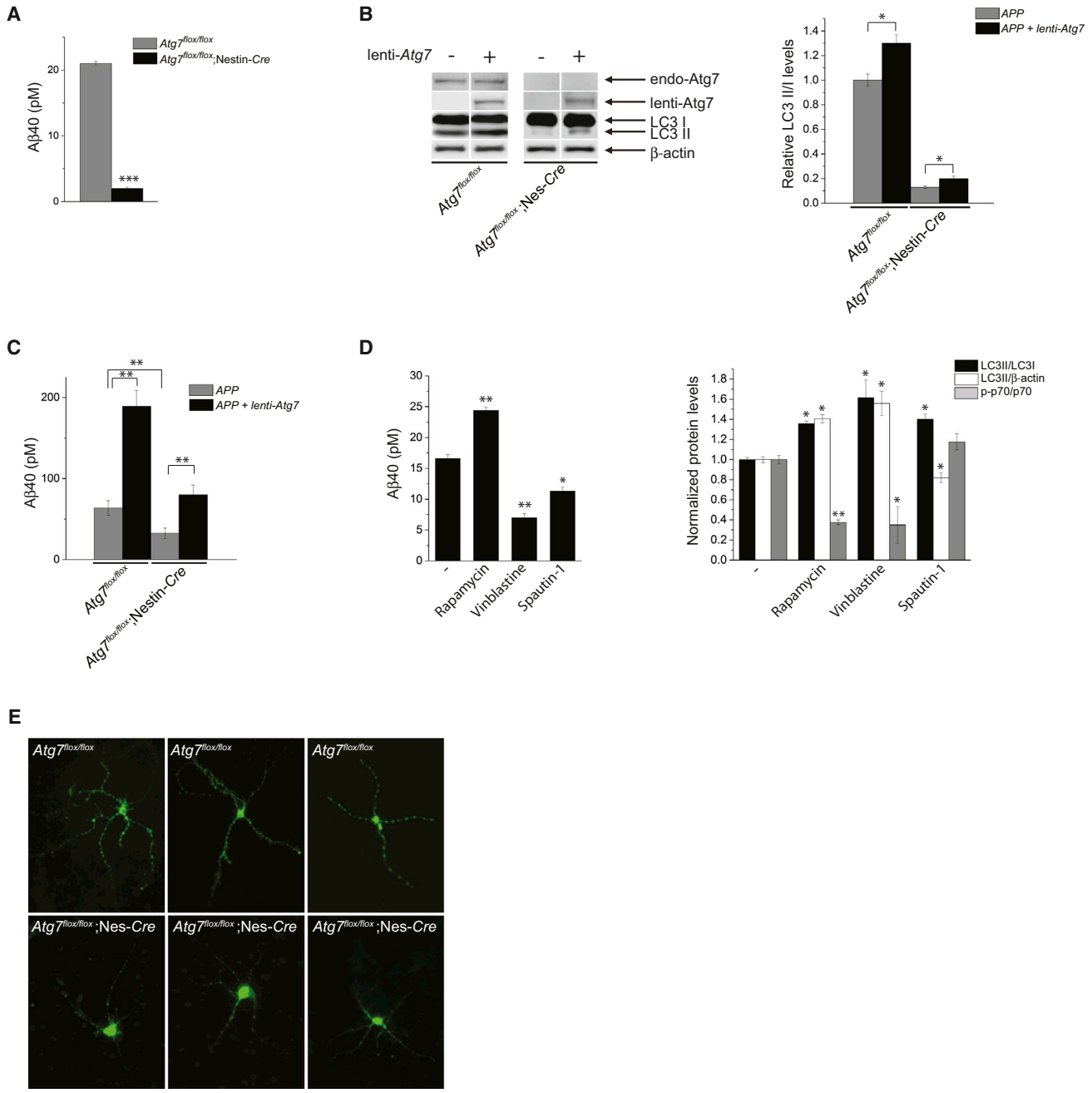

Figure 2. Autophagy Influences Aβ Secretion

(A) Release of endogenous Aβ from *Atg7*$^{flox/flox}$ and *Atg7*$^{flox/flox}$; Nes-*Cre* cortical/hippocampal primary neurons was determined by ELISA measurements of conditioned media (n = 3, ***p < 0.0001).

(B and C) Lenti-Atg7 expression in primary neurons activates autophagy and increases release of Aβ. Autophagy activation was measured by monitoring LC3 metabolism by quantitative western blot (n = 6, *p < 0.05, **p < 0.01).

(D) Aβ ELISA measurements of conditioned media from wild-type primary neurons infected with SFV-APP and treated with pharmacological compounds as indicated (n = 4, *p < 0.05, **p < 0.01). Activation and modulation of autophagy were determined by measuring LC3II/I, LC3II/β-actin and p-p70/p70 levels, respectively, by quantitative western blot (n = 6; *p < 0.05, **p < 0.01).

(E) *Atg7*$^{flox/flox}$ and *Atg7*$^{flox/flox}$; Nes-*Cre* primary neurons were infected with SFV-APP and stained for Aβ (Aβ40 antibody). Three representative neurons per genotype are shown.

Data are represented as mean ± SEM.

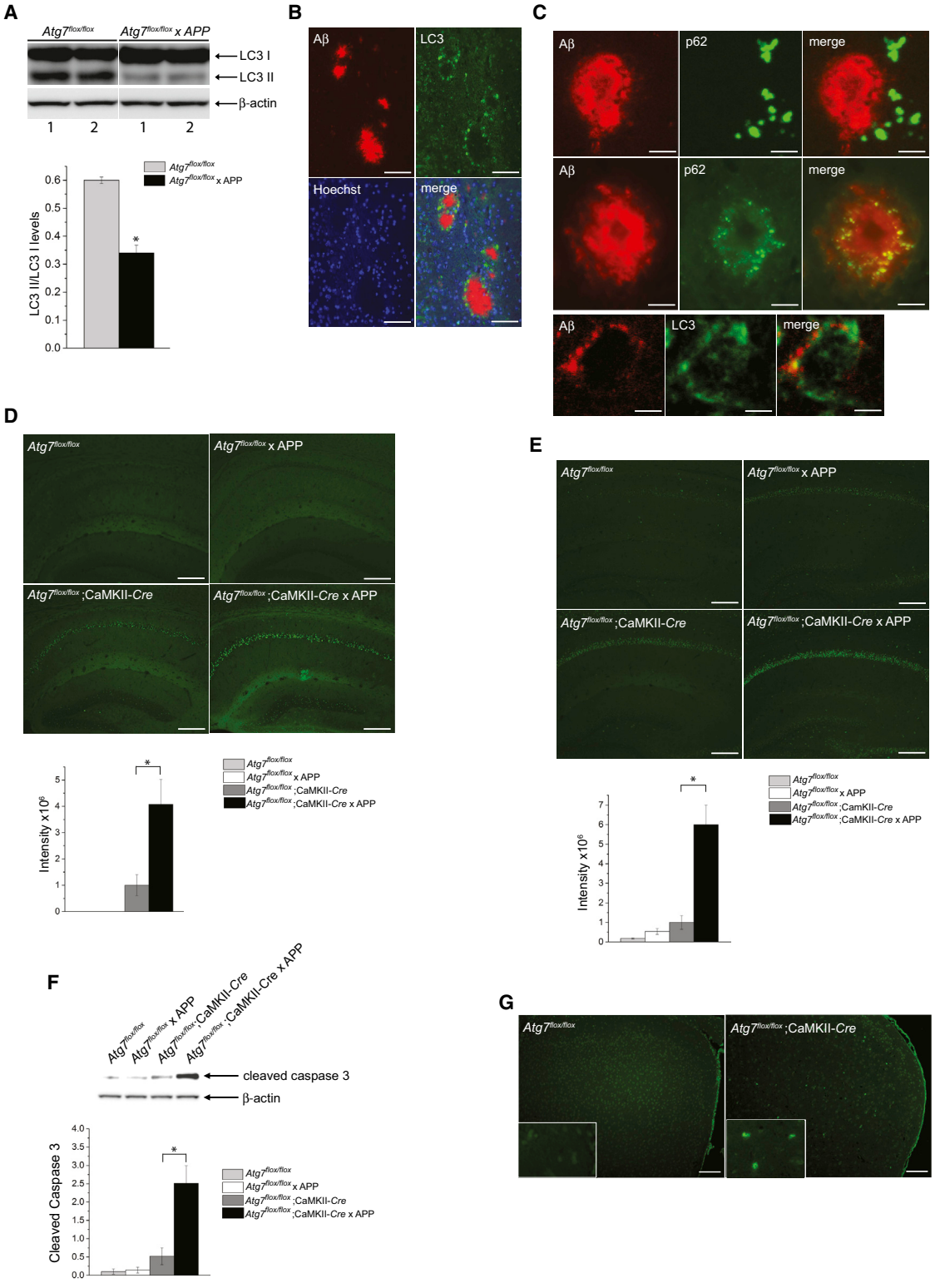

Figure 3. Amyloidosis Inhibits Autophagy and Activates Neurodegenerative Processes

(A) Western blot analysis of LC3 in cortical brain homogenates from *Atg7*$^{flox/flox}$ and *Atg7*$^{flox/flox}$ × APP mice (representative samples from two individuals per genotype are shown). LC3 immunoreactivity was quantified (n = 5, *p < 0.0005).

(B and C) Coimmunostaining of Aβ (4G8 antibody) and LC3 (B) and Aβ and p62 (C) using brain sections of 15-month-old *Atg7*$^{flox/flox}$ × APP mice.

(legend continued on next page)

through either exocytic or excretory mechanisms, and hence plays a key role in Aβ plaque formation.

Aβ Amyloidosis Inhibits Autophagy and Exacerbates Autophagy-Deficiency-Induced Neurodegeneration

Given that autophagy is impaired in AD, we investigated the in vivo effects of Aβ amyloidosis on autophagy in *Atg7*$^{flox/flox}$ × APP mice. We measured the levels of LC3I and LC3II in brain homogenates and found that LC3II levels were significantly reduced by 50% in *Atg7*$^{flox/flox}$ × APP mice compared to *Atg7*$^{flox/flox}$ mice, indicating that amyloidosis suppresses autophagy (Figure 3A; $p < 0.0005$). Furthermore, LC3 staining was markedly increased in the neuronal cells immediately surrounding the Aβ plaques, suggesting a direct local inhibitory effect of amyloidosis on autophagy (Figure 3B). In addition, LC3 colocalized in certain loci with intracellular Aβ (Figure 3C). A second indication of autophagy inhibition by amyloidosis is the accumulation of p62 found both in the vicinity of and inside the Aβ plaque (Figure 3C) closely resembling dystrophic neurites, although p62 staining did not directly overlap with phosphorylated tau (data not shown). These data suggest, in agreement with previous studies, an inhibitory effect of amyloidosis on autophagy.

The indication of autophagy-impaired neurons in *Atg7*$^{flox/flox}$ × APP mice and the fact that autophagy deficiency induces neurodegeneration (Komatsu et al., 2006, Inoue et al., 2012) prompted us to investigate neurodegeneration in the mutant mice. Although no apoptotic DNA fragmentation was found by TUNEL (data not shown), cleaved caspase-3 was detected in hippocampal brain homogenate by western blot and in CA1 pyramidal neurons by immunostaining of autophagy-deficient *Atg7*$^{flox/flox}$; CaMKII-*Cre* mice and was further enhanced in *Atg7*$^{flox/flox}$; CaMKII-*Cre* × APP mice (Figures 3D and 3F; $p < 0.01$). In addition, Fluoro-jade C-positive staining was observed in *Atg7*$^{flox/flox}$; CamKII-*Cre* mice (*Atg7*$^{flox/flox}$; CamKII-*Cre* × APP mice were omitted from the analysis because Fluoro-jade C stains Aβ) indicating activation of necrotic-mediated degeneration. Consistently, receptor-interacting serine/threonine-protein kinase 1 staining was detected in CA1 pyramidal cells of *Atg7*$^{flox/flox}$; CamKII-*Cre* mice and was significantly enhanced in *Atg7*$^{flox/flox}$; CamKII-*Cre* × APP mice (Figures 3E and 3G; $p < 0.01$). In summary, these data indicate that amyloidosis intensifies autophagy-deficiency-induced neurodegenerative processes.

To determine if activation of neurodegenerative processes leads to brain atrophy, we investigated the brains of the mutant mice by several means. First, a decrease in the wet weights of dissected cortical and hippocampal brain tissue was detected upon deletion of autophagy and the degeneration was further exacerbated by amyloidosis, accompanied by a significantly decreased body weight (Figure 4A; Figure S4A; $p < 0.01$). Consistently, hematoxylin and eosin (H&E) staining revealed a significant decrease in the size of hippocampus and cortical thickness (measured at posterior parietal associated area) in *Atg7*$^{flox/flox}$; CamKII-*Cre* × APP mice as compared to *Atg7*$^{flox/flox}$; CamKII-*Cre* mice (Figure 4B; $p < 0.05$). T2 magnetic resonance imaging (MRI) measurements confirmed a 22% decrease in hippocampal volume of *Atg7*$^{flox/flox}$; CamKII-*Cre* × APP mice as compared to *Atg7*$^{flox/flox}$ mice (Figure 4C; Figure S4B; $p < 0.005$) and a trend toward decreased hippocampal volume as compared to *Atg7*$^{flox/flox}$; CamKII-*Cre* mice. Cell counting revealed a 10% loss of p62-positive pyramidal neurons in CA1 of *Atg7*$^{flox/flox}$; CamKII-*Cre* × APP mice as compared to *Atg7*$^{flox/flox}$; CamKII-*Cre* mice (Figure 4D; $p < 0.05$). In conclusion, amyloidosis exacerbates the autophagy-deficiency-induced neurodegeneration and causes neuronal cell death.

Memory Impairment in Autophagy-Deficient Mice

To analyze the memory effects of intracellular Aβ accumulation and amyloidosis-exacerbated autophagy-deficiency-induced neurodegeneration in *Atg7*$^{flox/flox}$; CamKII-*Cre* × APP mice, we subjected 15-month-old littermates to Morris water maze. Whereas *Atg7*$^{flox/flox}$ mice efficiently learned to find the hidden platform, *Atg7*$^{flox/flox}$; CamKII-*Cre* × APP mice exhibited severe memory impairments (Figure 4E; $p < 0.005$) and performed significantly worse than *Atg7*$^{flox/flox}$ × APP mice ($p < 0.05$). The performance of autophagy-deficient *Atg7*$^{flox/flox}$; CamKII-*Cre* mice was not significantly different from that of *Atg7*$^{flox/flox}$ mice ($p = 0.28$). However, the improvement in learning was modest, suggesting that autophagy deficiency affects memory to some extent. In summary, these results indicate that impaired proteostasis and amyloidosis together severely affect memory either directly or by inducing neurodegeneration. Furthermore, the data highlight that extracellular Aβ plaques may not be a critical factor for severe memory impairment and support previous findings that intracellular Aβ is potentially neurotoxic.

DISCUSSION

In this study, we have investigated the in vivo role of autophagy, which is impaired in AD, in Aβ metabolism by analyzing neuron-specific autophagy-deficient APP mice. Surprisingly, and in contrast to the well-established degradative role of autophagy ending in lysosomal degradation, we found that autophagy influences the secretion of Aβ. These findings imply that autophagy directly affects two of the hallmarks in AD: intracellular Aβ accumulation and extracellular Aβ plaque formation (Figures 1 and 2).

Recently, a role for autophagy in protein secretion has emerged (reviewed in Deretic et al., 2012). Autophagy participates in nondegradative secretion of integral membrane proteins directly from endoplasmic reticulum (ER), through ER-to-Golgi-to plasma membrane (PM) secretory pathway or via secretory lysosomes. APP has previously been shown to be transported and processed to Aβ through the ER-Golgi-to-PM secretory pathway or transported unprocessed to PM, where Aβ is generated after endocytosis. Autophagosomes are sites of Aβ

(D and E) Immunostaining for cleaved caspase 3 (D) and RIPK1 (E) of 15-month-old brain sections with genotypes as indicated. The intensities were quantified ($n = 5$, $^*p < 0.01$).

(F) Quantitative western blot analysis of cleaved caspase 3 ($n = 3$, $^*p < 0.05$).

(G) Fluor-jade C staining of 15-month-old brain sections with indicated genotypes. Insets show 40× magnification.

Scale bar represents 50 μm (B), 25 μm (C, upper panel), 4 μm (C, lower panel), and 100 μm (D, E, and G). Data are represented as mean ± SEM.

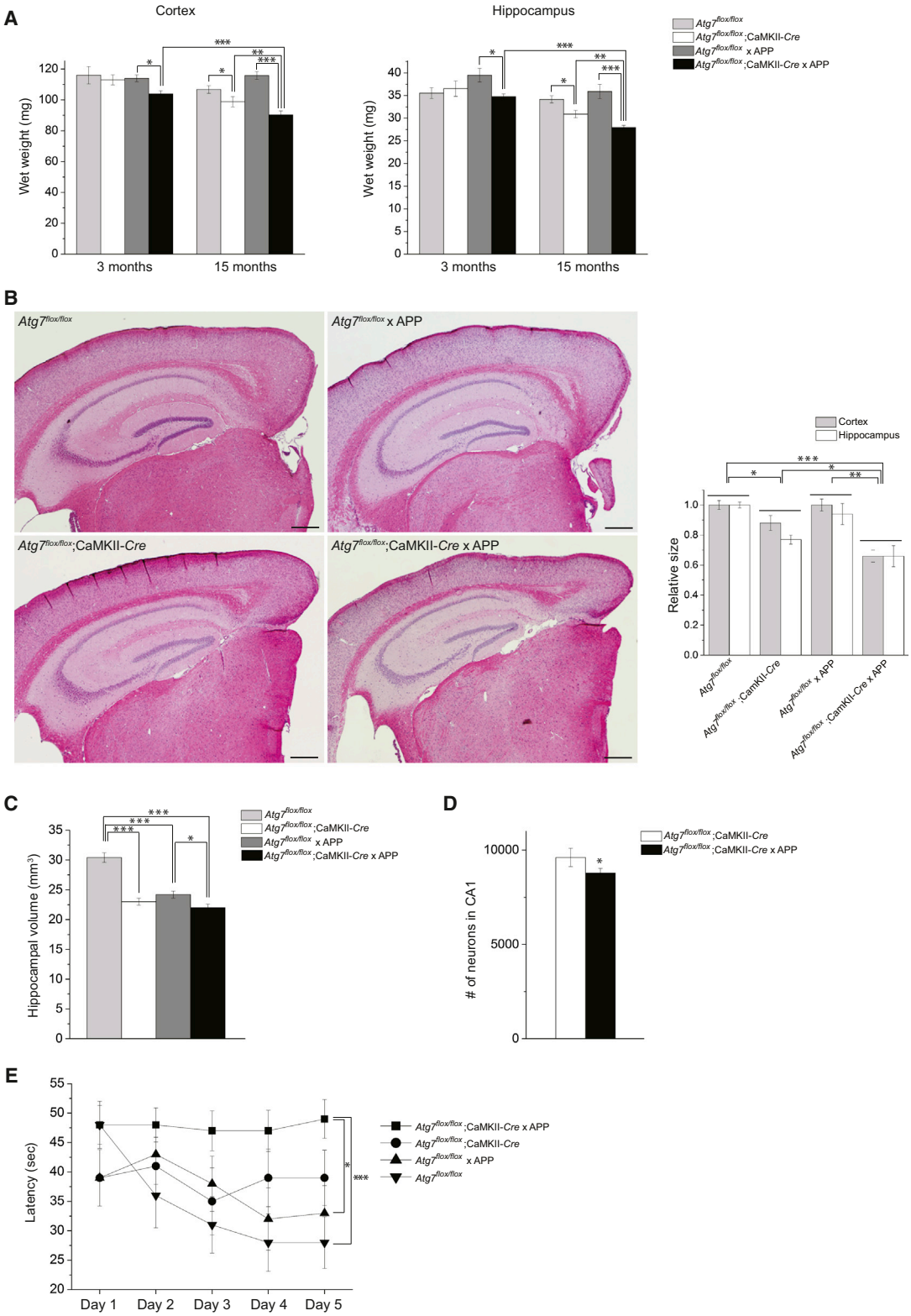

Figure 4. Amyloidosis Exacerbates Autophagy-Deficiency-Induced Neurodegeneration

(A) Wet weights of dissected brain tissue from 3- and 15-month-old mice with genotypes as indicated (n = 5/genotype).

(B) Representative sections stained by H&E from 15-month-old mice with genotypes as indicated. The cortical and hippocampal thickness were quantified.

(legend continued on next page)

generation; it remains to be determined if any of these secretory pathways is influenced by autophagy. In this context, it is noteworthy to mention that autophagosomes are formed at the ER-mitochondria contact site (Hamasaki et al., 2013). Because autophagosomes can fuse with endosomes at the late stage of autophagy, Aβ-containing endosomes could potentially be the source of Aβ released to extracellular space. However, it cannot be excluded that extracellular release of Aβ influenced by autophagy could be part of a general excretory mechanism for cellular waste, independent of the regulated secretory pathways.

If the increased number of autophagosomes observed in AD is due to increased autophagy, then it would result in increased Aβ secretion. On the other hand, if the autophagosomes accumulate due to impairment in the end stage of autophagosome clearance, intracellular Aβ levels would rise. Indeed, neurons in the AD brain exhibit intraneuronal Aβ accumulation, and recent data suggest that intracellular Aβ causes neurodegeneration by increased ER stress. We found that neurodegeneration induced by autophagy deficiency was exacerbated by amyloidosis and that these two pathologies, together with impaired proteostasis, caused severe memory impairment (Figures 3 and 4). The enhanced neurodegeneration and memory impairment could potentially be explained by the intracellular Aβ accumulation, given the sparse Aβ plaque load in *Atg7*$^{flox/flox}$; CamKII-*Cre* × APP mice, which would indicate that intracellular Aβ is toxic. More research is warranted to elucidate how intracellular Aβ mediates toxicity.

Administration of autophagy-activating rapamycin clears intracellular Aβ and improves cognition in the 3×Tg-AD mice (Caccamo et al., 2010), raising the question if such treatment is applicable to AD. Inducing autophagy would clear potentially neurotoxic intracellular Aβ at the expense of increased Aβ release. Hence, coadministration of an Aβ-lowering treatment would be needed to effectively prevent extracellular amyloidosis. In conclusion, our data establish that autophagy influences Aβ transport and release to the extracellular space and thereby directly affects Aβ plaque formation. Thus, autophagy plays a crucial role in AD pathology and could be a potential AD drug target.

EXPERIMENTAL PROCEDURES

Animals

Atg7$^{flox/flox}$ mice (Komatsu et al., 2005) were kindly provided by Dr. Keiji Tanaka (Tokyo Metropolitan Institute of Medical Science) and CamKII-*Cre* mice (Tsien et al., 1996) were kindly provided by Dr. Shigeyoshi Itohara (RIKEN Brain Science Institute). APP23 mice have been described previously (Sturchler-Pierrat et al., 1997). All animal experiments were carried out according to the guidelines of RIKEN Brain Science Institute.

Immunoblot Analysis

A total of 10 μg of brain homogenates was separated by SDS-PAGE, transferred to membranes, and probed with antibodies as listed in Table S1. For detection of cleaved caspase-3, the membrane was incubated with 1% glutaraldehyde in PBS before processing.

Histochemical and Immunohistochemical Analysis

Sections 4 μm (paraffin embedded) or 10 μm (fresh frozen) thick were stained with H&E, cresyl violet, toluidine blue, or fluoro-jade C (AG325, Chemicon), or immunostained using antibodies listed in Table S1. For Aβ immunostaining, tissue sections were treated with 90% formic acid for 5 min. Quantification was performed with MetaMorph imaging software (Universal Imaging). For the cell counting experiment, PFA-fixed sections 5 μm thick were collected from bregma −0.90 to −4.40 with 50 μm intervals and stained by p62 and Hoechst. p62-positive neurons were manually counted with blinded samples.

Primary Neuron Culture

Cortical/hippocampal neurons were prepared from embryonic day 17 to 18 (E17–E18) mouse embryos as previously described (Hama et al., 2001). Embryos from *Atg7*$^{flox/flox}$; Nes-*Cre* mice were separately genotyped. A total of 1.8 × 10^5 vital cells were plated in 24-well plates by trypan blue staining a 10 μl cell suspension and counting vital cells in a hemacytometer. After 10 days in vitro, endogenous Aβ levels in conditioned media were measured by ELISA by centrifugation of the media for 1 min at 3,000 rpm. Guanidin-HCl was added to prevent aggregation (final concentration 0.5 M) or the cells were infected with 10 μl semliki forest virus (SFV) expressing APP. Then, 24 hr postinfection, conditioned media were collected followed by Aβ ELISA measurement. Same conditions were applied for autophagy activation/inhibition experiments with rapamycin (2.7 nM, Sigma), vinblastine (50 μM, Sigma), and Spautin-1 (10 μM, BioVision Technologies) added to the media 23 hr postinfection to assure full effect of the compounds prior to Aβ measurements. The media was changed 24 hr postinfection to inhibitor-containing media. Three hours later, Aβ levels in conditioned media were measured by ELISA. The cells were collected in PBS, centrifuged, and dissolved in SDS sample buffer containing 0.1 M DTT for subsequent western blot analysis of APP expression analysis, to which Aβ levels were normalized.

Immunofluorescence

Primary neurons were infected with SFV-APP for 24 hr, fixed for 10 min in cold 4% paraformaldehyde and 0.1 M phosphate buffer, washed with PBS, blocked with 5% NGS and 1% saponin, and incubated with antibodies overnight. Wash buffer and antibodies dilutions contained 1% saponin.

ELISA

TS and GS Aβ from cortical and hippocampal homogenates (Iwata et al., 2004) and conditioned media were determined by ELISA (Wako or IBL) according to the manufacturer's instructions.

Morris Water Maze

Fifteen-month-old littermates (*Atg7*$^{flox/flox}$, *Atg7*$^{flox/flox}$; CaMKII-*Cre*, *Atg7*$^{flox/flox}$ × APP, *Atg7*$^{flox/flox}$; CaMKII-*Cre* × APP, n = 10) were acclimatized to the behavioral laboratory 3 days before tests. The light condition was 12 hr:12 hr (lights on at 8:00 am). Tests were performed from 9:30 am to 3:30 pm. Each mouse was assessed in two training sessions per day. Mice had ad libitum access to food and water (except during the tests).

MRI

Fifteen-month-old *Atg7*$^{flox/flox}$, *Atg7*$^{flox/flox}$; CaMKII-*Cre*, *Atg7*$^{flox/flox}$ × APP, *Atg7*$^{flox/flox}$; CaMKII-*Cre* × APP (n = 3/genotype) mice were anesthetized with isoflurane (1.5%–2% in air) and mounted in a stereotaxic apparatus. The depth of anesthesia was monitored with a breathing sensor. MRI scans of the whole brain were performed with a vertical-bore 9.4 T Bruker AVANCE 400WB imaging spectrometer with a 250 mT m^{-1} actively shielded imaging gradient insert (Bruker BioSpin) controlled by Paravision software. T2-weighted images were obtained with the following parameter settings: matrix dimensions = 256 × 256 × 29, TE = 53.5 ms, TR = 434.2 ms, flip angle = 180

(C) Hippocampal volume was calculated from T2 MRI data.
(D) Cell counting of p62-positive neurons in CA1 of 20-month-old *Atg7*$^{flox/flox}$; CamKII-*Cre* and *Atg7*$^{flox/flox}$; CamKII-*Cre* × APP mice.
(E) Morris water maze was performed with 15-month-old littermates with genotypes as indicated (n = 10). The performance on day 5 was analyzed by ANOVA followed by Tukey's post hoc test.
Scale bar represents 500 μm. Data are represented as mean ± SEM. *p < 0.05, **p < 0.01, ***p < 0.005. See also Figure S4.

degrees, FOV = 16 × 16 × 0.5. A total of 29 high-resolution coronal slices of the whole brain were collected. Total scanning time was 60 min per individual. Within the 29 MRI slices, 8 slices contained the hippocampal formation (from bregma −0.90 to −4.40), which was manually selected by the paintbrush tool and used for the volumetric calculation of hippocampus using InsightITK-Snap software version 2.2.0.

Statistical Analysis

Data were analyzed by Student's t test if not stated otherwise and are presented as average ± SEM.

SUPPLEMENTAL INFORMATION

Supplemental Information includes four figures and one table and can be found with this article online at http://dx.doi.org/10.1016/j.celrep.2013.08.042.

ACKNOWLEDGMENTS

We thank Keiji Tanaka and Shigeyoshi Itohara for generously providing *Atg7*$^{flox/flox}$ and CamKII-*Cre* mice, respectively. We acknowledge the members of the PNS lab, Jiro Takano, Ko Sato, Kenichi Nagata, Naomasa Kakiya, Shoko Hashimoto, Hayato Isshiki, Kaori Tsukakoshi, Karin Sörgjerd, Emi Hosoki, Ryo Fujioka, Naomi Yamazaki, Yuya Tomita, and Yukiko Nagai. We appreciate the kind gift of the HDAC6 antibody from Tso-Pang Yao. This project was financially supported by research grants from Swedish Research Council, Sweden; RIKEN Brain Science Institute; Ministry of Education, Sports, Science and Technology, Japan; and Ministry of Health, Labour and Welfare, Japan.

Received: November 9, 2012
Revised: July 17, 2013
Accepted: August 23, 2013
Published: October 3, 2013

REFERENCES

Boland, B., Kumar, A., Lee, S., Platt, F.M., Wegiel, J., Yu, W.H., and Nixon, R.A. (2008). Autophagy induction and autophagosome clearance in neurons: relationship to autophagic pathology in Alzheimer's disease. J. Neurosci. *28*, 6926–6937.

Boland, B., Smith, D.A., Mooney, D., Jung, S.S., Walsh, D.M., and Platt, F.M. (2010). Macroautophagy is not directly involved in the metabolism of amyloid precursor protein. J. Biol. Chem. *285*, 37415–37426.

Caccamo, A., Majumder, S., Richardson, A., Strong, R., and Oddo, S. (2010). Molecular interplay between mammalian target of rapamycin (mTOR), amyloid-β, and Tau: effects on cognitive impairments. J. Biol. Chem. *285*, 13107–13120.

Deretic, V., Jiang, S., and Dupont, N. (2012). Autophagy intersections with conventional and unconventional secretion in tissue development, remodeling and inflammation. Trends Cell Biol. *22*, 397–406.

Hama, E., Shirotani, K., Masumoto, H., Sekine-Aizawa, Y., Aizawa, H., and Saido, T.C. (2001). Clearance of extracellular and cell-associated amyloid β peptide through viral expression of neprilysin in primary neurons. J. Biochem. *130*, 721–726.

Hamasaki, M., Furuta, N., Matsuda, A., Nezu, A., Yamamoto, A., Fujita, N., Oomori, H., Noda, T., Haraguchi, T., Hiraoka, Y., et al. (2013). Autophagosomes form at ER-mitochondria contact sites. Nature *495*, 389–393.

Hara, T., Nakamura, K., Matsui, M., Yamamoto, A., Nakahara, Y., Suzuki-Migishima, R., Yokoyama, M., Mishima, K., Saito, I., Okano, H., and Mizushima, N. (2006). Suppression of basal autophagy in neural cells causes neurodegenerative disease in mice. Nature *441*, 885–889.

Harris, H., and Rubinsztein, D.C. (2012). Control of autophagy as a therapy for neurodegenerative disease. Nat. Rev. Neurol. *8*, 108–117.

Inoue, K., Rispoli, J., Kaphzan, H., Klann, E., Chen, E.I., Kim, J., Komatsu, M., and Abeliovich, A. (2012). Macroautophagy deficiency mediates age-dependent neurodegeneration through a phospho-tau pathway. Mol. Neurodegener. *7*, 48.

Iwata, N., Mizukami, H., Shirotani, K., Takaki, Y., Muramatsu, S.-i., Lu, B., Gerard, N.P., Gerard, C., Ozawa, K., and Saido, T.C. (2004). Presynaptic localization of neprilysin contributes to efficient clearance of amyloid-β peptide in mouse brain. J. Neurosci. *24*, 991–998.

Jaeger, P.A., Pickford, F., Sun, C.-H., Lucin, K.M., Masliah, E., and Wyss-Coray, T. (2010). Regulation of amyloid precursor protein processing by the Beclin 1 complex. PLoS ONE *5*, e11102.

Komatsu, M., Waguri, S., Ueno, T., Iwata, J., Murata, S., Tanida, I., Ezaki, J., Mizushima, N., Ohsumi, Y., Uchiyama, Y., et al. (2005). Impairment of starvation-induced and constitutive autophagy in Atg7-deficient mice. J. Cell Biol. *169*, 425–434.

Komatsu, M., Waguri, S., Chiba, T., Murata, S., Iwata, J.-i., Tanida, I., Ueno, T., Koike, M., Uchiyama, Y., Kominami, E., and Tanaka, K. (2006). Loss of autophagy in the central nervous system causes neurodegeneration in mice. Nature *441*, 880–884.

Komatsu, M., Wang, Q.J., Holstein, G.R., Friedrich, V.L., Jr., Iwata, J.-i., Kominami, E., Chait, B.T., Tanaka, K., and Yue, Z. (2007). Essential role for autophagy protein Atg7 in the maintenance of axonal homeostasis and the prevention of axonal degeneration. Proc. Natl. Acad. Sci. USA *104*, 14489–14494.

LaFerla, F.M., Green, K.N., and Oddo, S. (2007). Intracellular amyloid-beta in Alzheimer's disease. Nat. Rev. Neurosci. *8*, 499–509.

Lee, J.-H., Yu, W.H., Kumar, A., Lee, S., Mohan, P.S., Peterhoff, C.M., Wolfe, D.M., Martinez-Vicente, M., Massey, A.C., Sovak, G., et al. (2010a). Lysosomal proteolysis and autophagy require presenilin 1 and are disrupted by Alzheimer-related PS1 mutations. Cell *141*, 1146–1158.

Majumder, S., Richardson, A., Strong, R., and Oddo, S. (2011). Inducing autophagy by rapamycin before, but not after, the formation of plaques and tangles ameliorates cognitive deficits. PLoS ONE *6*, e25416.

Mizushima, N., and Komatsu, M. (2011). Autophagy: renovation of cells and tissues. Cell *147*, 728–741.

Nixon, R.A. (2007). Autophagy, amyloidogenesis and Alzheimer disease. J. Cell Sci. *120*, 4081–4091.

Pickford, F.M.E., Masliah, E., Britschgi, M., Lucin, K., Narasimhan, R., Jaeger, P.A., Small, S., Spencer, B., Rockenstein, E., Levine, B., and Wyss-Coray, T. (2008). The autophagy-related protein beclin 1 shows reduced expression in early Alzheimer disease and regulates amyloid β accumulation in mice. J. Clin. Invest. *118*, 2190–2199.

Saido, T.C., Yokota, M., Maruyama, K., Yamao-Harigaya, W., Tani, E., Ihara, Y., and Kawashima, S. (1994). Spatial resolution of the primary beta-amyloidogenic process induced in postischemic hippocampus. J. Biol. Chem. *269*, 15253–15257.

Sturchler-Pierrat, C., Abramowski, D., Duke, M., Wiederhold, K.-H., Mistl, C., Rothacher, S., Ledermann, B., Bürki, K., Frey, P., Paganetti, P.A., et al. (1997). Two amyloid precursor protein transgenic mouse models with Alzheimer disease-like pathology. Proc. Natl. Acad. Sci. USA *94*, 13287–13292.

Tsien, J.Z., Chen, D.F., Gerber, D., Tom, C., Mercer, E.H., Anderson, D.J., Mayford, M., Kandel, E.R., and Tonegawa, S. (1996). Subregion- and cell type-restricted gene knockout in mouse brain. Cell *87*, 1317–1326.

Wirths, O., and Bayer, T.A. (2012). Intraneuronal Aβ accumulation and neurodegeneration: lessons from transgenic models. Life Sci. *91*, 1148–1152. http://dx.doi.org/10.1016/j.lfs.2012.02.001.

Yang, D.-S., Stavrides, P., Mohan, P.S., Kaushik, S., Kumar, A., Ohno, M., Schmidt, S.D., Wesson, D., Bandyopadhyay, U., Jiang, Y., et al. (2011). Reversal of autophagy dysfunction in the TgCRND8 mouse model of Alzheimer's disease ameliorates amyloid pathologies and memory deficits. Brain *134*, 258–277.

Yu, W.H., Cuervo, A.M., Kumar, A., Peterhoff, C.M., Schmidt, S.D., Lee, J.-H., Mohan, P.S., Mercken, M., Farmery, M.R., Tjernberg, L.O., et al. (2005). Macroautophagy—a novel β-amyloid peptide-generating pathway activated in Alzheimer's disease. J. Cell Biol. *171*, 87–98.

Zheng, L., Terman, A., Hallbeck, M., Dehvari, N., Cowburn, R.F., Benedikz, E., Kågedal, K., Cedazo-Minguez, A., and Marcusson, J. (2011). Macroautophagy-generated increase of lysosomal amyloid β-protein mediates oxidant-induced apoptosis of cultured neuroblastoma cells. Autophagy *7*, 1528–1545.